

Rotational analysis of the origin and the inversion bands of the $S_1 \leftarrow S_0$ spectrum of acetaldehyde

Erko Jalviste^{a)}

Institute of Physics, University of Tartu, Riia 142, 51014 Tartu, Estonia

Giel Berden^{b)}

Department of Molecular and Laser Physics, University of Nijmegen, Toernooiveld, 6525 ED Nijmegen, The Netherlands

Marcel Drabbels

Department of Chemistry, Swiss Federal Institute of Technology Lausanne (EPFL), CH-1015 Lausanne, Switzerland

Alec M. Wodtke

Department of Chemistry, University of California at Santa Barbara, Santa Barbara, California 93106

(Received 13 December 2000; accepted 28 February 2001)

Fully rotationally resolved spectra of the two lowest-frequency bands (the origin (0_0^0) and the inversion (14_0^1) band) of the $S_1(n\pi^*) \leftarrow S_0$ transition of jet-cooled ($T_{\text{rot}} \approx 6$ K) acetaldehyde, CH_3CHO , have been recorded with a resolution of $\approx 0.01 \text{ cm}^{-1}$ using a pulsed dye amplified continuous wave (cw) laser. In modeling the spectra a nonperturbative solution of the rotational-torsional coupling problem was used, but the torsion-inversion and the rotation-inversion couplings were neglected. All the lines of the origin band were reproduced with a model using the same rotational-torsional Hamiltonian for the ground- and excited electronic state. The inversion band could not be described with this model, since the ordering of the torsional levels in the excited state is reversed. The measured spectrum was reproduced by using a rigid asymmetric rotor Hamiltonian for the two torsional levels in the excited state. Some rotational levels of 0^0 and 14^1 states were found to be shifted from their predicted energy values. These shifts were explained by an accidental resonance between the excited singlet level and some higher rovibronic triplet level. The relative intensities of the *ab*-type and *c*-type torsional subbands and the Herzberg-Teller-induced transition dipole moment direction, characterizing the *ab*-type subband, were determined by an intensity fit. © 2001 American Institute of Physics. [DOI: 10.1063/1.1366643]

I. INTRODUCTION

Acetaldehyde (CH_3CHO) in its ground state is one of the simplest and best-studied prototype systems for investigating the spectroscopic manifestations of the coupling between the overall rotation of the molecule and the methyl torsion large amplitude motion.

Rotational-torsional coupling terms were already introduced into the Hamiltonian in the early microwave study of Kilb *et al.*¹ The measurement of additional microwave and far infrared transitions together with better (faster) computing possibilities enabled improved rotational-torsional analysis.² Further developments in theory led to modern global fitting models,³⁻⁸ which are able to fit thousands of lines belonging to transitions between states with torsional quantum numbers $v_t \leq 4$, and rotational quantum numbers $J \leq 26$ and $K_a \leq 14$. The number of parameters in these global fits is quite high; up to 60 parameters were needed to fit the transitions within their observed uncertainty.

The $n\pi^*$ -type $S_1 \leftarrow S_0$ electronic transition, whose vi-

bronic bands cover the near UV spectral region (350–250 nm), provides access to the first excited singlet state of acetaldehyde. Owing to the out-of-CCO-plane equilibrium position of the aldehydic hydrogen in the S_1 state, the inversion (wagging) vibration of this atom with respect to the CCO plane is the second large amplitude motion besides the methyl torsion.

Vibronic analysis of room-temperature gas cell absorption and fluorescence spectra revealed evidence of the methyl conformational change as well as the double-minimum character of the excited state inversion potential.^{9,10} It was also established that the excited state methyl torsional barrier increases upon electronic excitation. However, the analysis of room-temperature spectra was severely limited by congestion of many bands.

In the early 80's Noble *et al.*^{11,12} and Baba *et al.*¹³ recorded the laser-induced fluorescence excitation spectra of several acetaldehyde isotopomers in a supersonic jet. Due to the cooling of the vibrational and rotational degrees of freedom, the 0_0^0 band was unambiguously identified. Assignments were proposed for torsional-vibrational bands up to 1700 cm^{-1} above the origin band. Essential to establishing the band assignments was the rotational contour analysis, by which the dominant type of the rotational spectrum (*ab* or *c*

^{a)}Author to whom correspondence should be addressed. Electronic mail: erko@fi.tartu.ee

^{b)}Present address: FOM-Institute for Plasma Physics Rijnhuizen, Postbox 1207, 3430 BE Nieuwegein, The Netherlands.

type) was determined. Furthermore, the methyl conformational change and the out-of-plane movement of acetyl hydrogen upon electronic excitation were confirmed, and reliable parameters of one-dimensional model potentials describing the torsion and wagging large amplitude motions in the S_1 were deduced.

Weersink *et al.*¹⁴ developed a torsion–inversion coupling model for the excited state and applied this model to the spectra of Noble *et al.*¹² They deduced a two-dimensional potential energy surface, characterizing these large amplitude motions and the structure parameters corresponding to the minima of the potential. Additionally, Weersink *et al.*¹⁴ clearly explained the physical nature of the *ab*- and *c*-type transitions to the excited state torsion–inversion levels.

Price *et al.*¹⁵ obtained excited state rotational constants of the CH_3CHO and CH_3CDO isotopomers from a rotational fit of their origin band spectra of jet-cooled acetaldehyde. The experimental resolution was $\approx 0.22 \text{ cm}^{-1}$, too low to resolve the individual rotational lines. The spectra were described with a simple rigid rotor Hamiltonian. From the rotational constants an approximate excited state geometry was determined.

Subsequent achievements, reflected in a series of publications of Liu *et al.*,^{16–18} were based on the use of a pulse amplified cw dye laser system, with 0.005 cm^{-1} laser linewidth. Analysis of the rotationally resolved spectra of selected $S_1 \leftarrow S_0$ vibronic bands, carried out with a rigid asymmetric top model, yielded precise frequencies of the band origins and corresponding rotational constants. The band origin frequencies have been fit to a torsion–wagging–CCO–bending model (substantially different from that of Weersink *et al.*¹⁴), resulting in a refined set of potential hypersurface and kinetic parameters characterizing these three modes.

In contrast to the very detailed global analysis of the ground-state data of acetaldehyde,^{6–8} to the best of our knowledge no reports exist where the coupling between overall rotation and methyl torsion is consistently taken into account in the rotational analysis of the $S_1 \leftarrow S_0$ electronic bands. This work attempts to fill this gap for the two lowest-frequency vibronic bands of $S_1 \leftarrow S_0$ transition, the origin and the inversion band. Rotationally resolved excitation spectra of jet-cooled acetaldehyde are measured with a pulse-amplified cw laser system and analyzed with frequency as well as with intensity fitting techniques.^{19,20}

II. EXPERIMENT

A molecular beam of acetaldehyde is formed by expanding 1% acetaldehyde in He (for the origin band) or 5% acetaldehyde in Ar (for the inversion band) through a pulsed valve with an orifice of 0.8 mm diameter into a vacuum chamber. For He beams, a backing pressure of 5 atm is applied. When Ar is used as the carrier gas, the backing pressure had to be lowered to 2 atm to avoid cluster formation. The molecular beam is crossed by a laser beam approximately 7 cm downstream of the nozzle. As excitation light source, a pulsed dye amplifier system is employed. The output of an Ar ion pumped ring dye laser (Coherent CR699), operated on DCM dye, is amplified in three stages by the

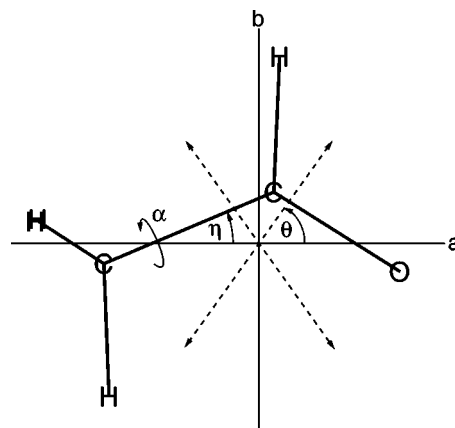


FIG. 1. Geometrical structure of acetaldehyde in the ground state and the orientation of principal inertial axes. The leftmost double H label marks the two out-of-CCO-plane methyl hydrogens. Two alternative directions of Herzberg–Teller-induced transition moment responsible for hybrid *ab*-type subbands in the electronic spectra are marked by arrows.

second harmonic of a Q-switched Nd-YAG laser (Lumonics HY600). The amplified radiation is frequency doubled in a KDP crystal to yield UV light around 335 nm with a pulse energy of typically $\approx 2 \text{ mJ}$ and a Fourier transform limited bandwidth of 0.006 cm^{-1} . For absolute frequency calibration the I_2 absorption spectrum^{21,22} is recorded along with the excitation spectrum of acetaldehyde. For relative frequency calibration transmission fringes are recorded with pressure and temperature stabilized Fabry–Perot interferometer with free spectral range 500.4(1) MHz. The fluorescence from the S_1 state to the ground state is collected by a $f/0.7$ quartz lens system and imaged onto a photomultiplier tube (Hamamatsu R212). In order to reduce the scattered light an L-400 cutoff filter is placed in front of the photomultiplier. The signals from the photomultiplier are processed by a digital oscilloscope (LeCroy 9430) and a boxcar integrator (SRS 250) interfaced with a computer.

III. THEORY

A. The subbands of the origin and the inversion band

In its ground state acetaldehyde is planar (except for the two methyl hydrogens). The third methyl hydrogen is eclipsed with respect to the carbonyl group (see Fig. 1). A threefold barrier for methyl torsion (ν_{15}) gives rise to a_1 , a_2 , and e torsional levels, designated by the species of G_6 molecular symmetry group. Due to a barrier height of 400 cm^{-1} the two lowest torsional levels with $\nu_t=0$, marked by $0a_1$ and $0e$, are separated by 0.07 cm^{-1} (see Fig. 2).

The equilibrium geometry in the S_1 state is significantly different from that of the ground state. The methyl group is rotated by an angle somewhat less than 60° (59.9° in Ref. 18, but 54° in Ref. 14), and the aldehydic hydrogen is bent out of the CCO plane by 35° .^{17,18,14} The nearly 60° conformational change of the methyl group gives rise to a long torsional progression in the excitation spectrum. The inversion (wagging, ν_{14}) motion of aldehydic hydrogen in the S_1 state can be described by a symmetric double-minimum potential, whose local maximum corresponds to the planar configura-

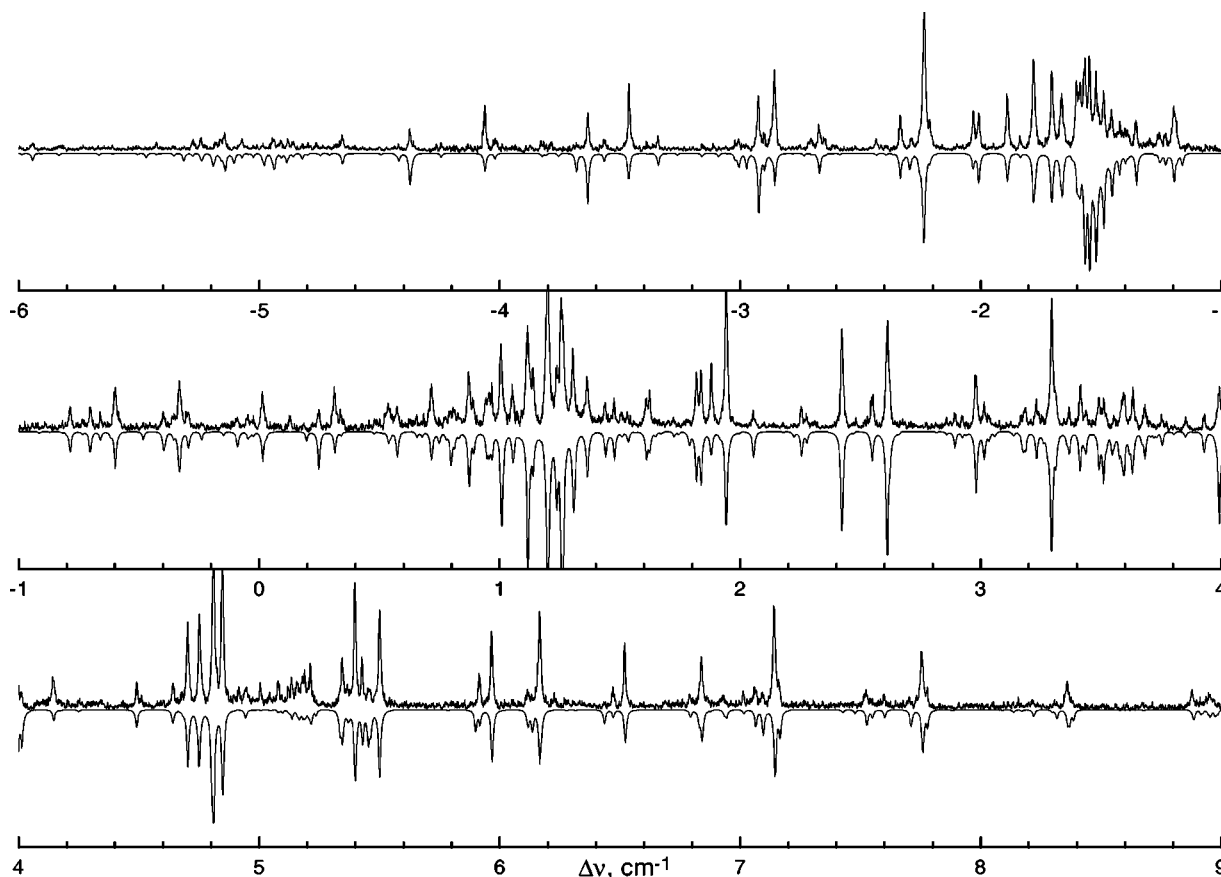


FIG. 3. Observed spectrum (upper trace) and simulated spectrum (lower trace) of the 0_0^0 band of acetaldehyde. The origin of the $0a_1-0a_1$ subband, marked in the figure at 0 cm^{-1} , is at $29\,769.046(6)\text{ cm}^{-1}$.

We use the axis convention, where η , ρ_a , and ρ_b are positive⁷ (see Fig. 1).

The Hamiltonian matrix is set up in a rotational-torsional basis consisting of the products of Wang-type rotational basis functions and one-dimensional free internal rotation sine-cosine-type basis functions as in the work of Huber *et al.*²⁸ The matrix elements for an equivalent, but differently parameterized Hamiltonian are given in Table III of that work. The Hamiltonian factorizes into blocks of overall symmetry a_1 , a_2 , and e , which are diagonalized separately for each J value. From the resulting eigenvalues and eigenvectors, only those corresponding to the torsional ground state, $v_t=0$, were selected.

The transition strength $S_{\psi'\psi''}$ between given RT levels of S_1 and S_0 state can be expressed by^{20,24,28}

$$S_{\psi'\psi''} \propto \mu_a^2 |\langle \psi' | \Phi_{Za} | \psi'' \rangle|^2 + \mu_b^2 |\langle \psi' | \Phi_{Zb} | \psi'' \rangle|^2 + 2\mu_a\mu_b \langle \psi' | \Phi_{Za} | \psi'' \rangle \langle \psi' | \Phi_{Zb} | \psi'' \rangle + \mu_c^2 |\langle \psi' | \Phi_{Zc} | \psi'' \rangle|^2, \quad (4)$$

where $|\psi\rangle$ is the RT eigenfunction, $\mu_a = \mu \cos \theta$, and $\mu_b = \mu \sin \theta$. The double and single prime denote the ground- and excited state, respectively, μ is the absolute value of the transition dipole moment, θ is the angle of the transition moment vector with respect to the a axis, and Φ_{Za} , Φ_{Zb} , and Φ_{Zc} are the direction cosines between the laboratory Z axis and the molecular a , b , and c axis, respectively. The first

three terms are nonzero for ab -type subbands and the last term is nonzero for c -type subbands. The absence of the cross terms $\propto \mu_a\mu_c$ and $\propto \mu_b\mu_c$ in Eq. (4) follows from the assumed symmetry of acetaldehyde with respect to the ab plane.

The line strength factors $S_{\psi'\psi''}$ are calculated by properly combining the expansion coefficients of $|\psi'\rangle$ to the excited-state RT basis, the expansion coefficients of $|\psi''\rangle$ to the ground-state RT basis, and the direction cosine matrix elements between the excited- and ground-state basis functions [see Eq. (8) in Ref. 28]. To obtain the line intensities the line strength factors are subsequently weighted by the Boltzmann factor and by the intensity weight factor of the subband to which the line belongs (*vide infra*). In order to take into account the 60° methyl conformational change on excitation the sign of either V_3' or V_3'' was set to negative.²⁸

A detailed description of the theory used here in the analysis of the electronic bands, its limitations, and its connections with other authors' work will be given elsewhere.²⁹

IV. RESULTS

The rotationally resolved spectra of the 0_0^0 band and the 14_0^1 band of the $S_1 \leftarrow S_0$ transition of acetaldehyde are shown in the upper traces of Figs. 3 and 4. The spectral resolution of the inversion band (0.008 cm^{-1}) is better than that of the origin band (0.012 cm^{-1}) because the origin band was mea-

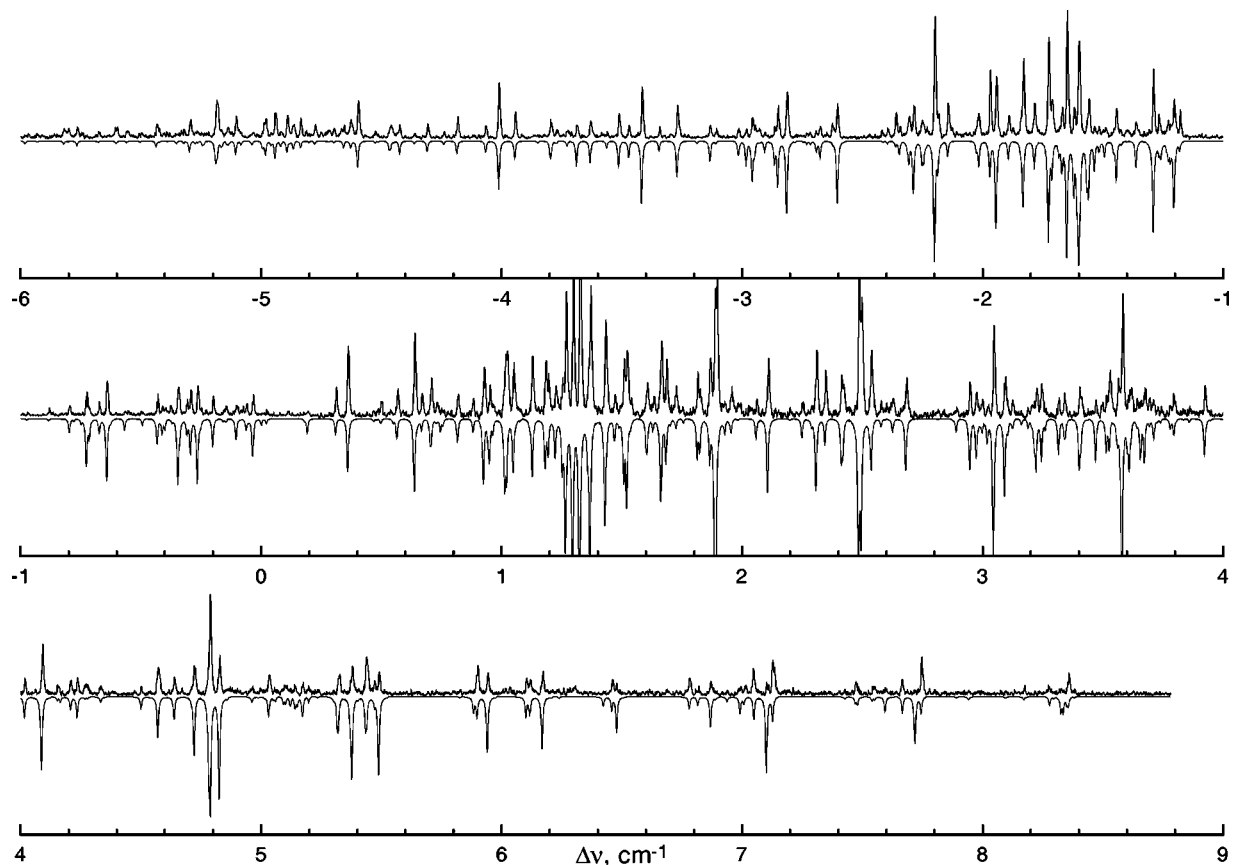


FIG. 4. Observed spectrum (upper trace) and simulated spectrum (lower trace) of the 14_0^1 band of acetaldehyde. The origin of the $0a_1-0a_1$ subband, marked in the figure at 0 cm^{-1} , is at $29\,803.420(7)\text{ cm}^{-1}$.

sured while acetaldehyde was seeded in helium, whereas the inversion band was measured with argon as a seeding gas.

The analysis of these spectra started by determining the ground-state molecular constants from ground-state data available in the literature. Then, we have made an assignment of the features in the electronic spectra, followed by a fit of frequencies of the assigned lines which provided us the molecular constants of the excited state. Finally, the intensities of the spectral lines are analyzed in order to extract additional information, like the relative intensities of the subbands.

A. Frequency analysis: The microwave spectrum

Although much effort has been devoted to the ground-state analysis, resulting in large sets of molecular constants, we could not use the published constants. The reason is that in the case of acetaldehyde the constants depend considerably on the model Hamiltonian and the number and type of transitions included into the fit. The larger the number of lines included in the analysis, the more sophisticated a model is necessary to fit all line frequencies within a given precision. This explains the variety of values found in the literature.

For our analysis, we included all the observed microwave transitions between the rotational sublevels of $v_i=0$ torsional level with $J''\leq 8$ and $J'\leq 9$ from Ref. 7 into the fit ($1580a_1-0a_1$ and $1530e-0e$ lines). It should be kept in

mind that here $0a_1-0a_1$ or $0e-0e$ denote the rotational transitions, whose final and initial state belongs to the same torsional $0a_1$ or $0e$ level of the S_0 state, respectively. Apart from the observed microwave transition frequencies, three far infrared torsional band origin frequencies were included: the $1a_1\leftarrow 0a_1$ at 143.7428 cm^{-1} , the $2a_1\leftarrow 1a_1$ at 110.2124 cm^{-1} , and the $1e\leftarrow 0e$ at 141.9237 cm^{-1} . These far infrared band origin frequencies were deduced by combining known frequencies of measured far infrared and microwave lines.⁸

As a compromise between model simplicity (fewer fit parameters) and the precision of the fit, we used, apart from the rotational and torsional constants, the distortion parameters Δ_J , Δ_{JK} , Δ_K , and δ_k as fit variables, but δ_J was kept fixed to zero. The distortion terms of the Hamiltonian are defined in a standard way [see Eq. (1) in Ref. 24]. A trial fit with variable δ_J yielded zero value for this parameter within its error limits. This selection of fit parameters enabled us to fit most of the microwave lines within 5 MHz precision. The root-mean-square standard deviation of the fit was 0.68 MHz ($2.3\times 10^{-5}\text{ cm}^{-1}$). To save on computing time, the size of the basis, given by the maximum allowed values of J and of the free internal rotation quantum number m , was limited to $J_{\max}=9$ and $m_{\max}=18$. For $m_{\max}=18$ the error of the torsional basis truncation was negligible, <0.05 MHz even for the $J,K_a,K_c=9,9,0$ level of the $0e$ species. The ground-state molecular constants obtained from our microwave fit are listed in the first column of Table I.

TABLE I. Molecular constants of the ground state (0_0), and electronically excited states 0^0 and 14^1 . Abbreviations: 0. means that this parameter is fixed to zero, g.s. means that the parameter is fixed to its ground-state value, and n.a. means that it is not a parameter. See the text for details.

	$0_0(S_0)$	$0^0(S_1)$	$14^1(S_1)$		
A	1.888 360(7)	1.601 91(7)	$A'_a = 1.597\ 60(8)$, $A'_e = 1.598\ 01(7)$	cm^{-1}	a
B	0.339 202 0(13)	0.338 638(21)	0.338 801(14)	cm^{-1}	
C	0.303 289 0(13)	0.296 450(16)	0.297 339(11)	cm^{-1}	
Δ_J	$0.263(13) \times 10^{-6}$	0.	0.	cm^{-1}	
Δ_{JK}	$-1.42(6) \times 10^{-6}$	0.	0.	cm^{-1}	
Δ_K	$23.48(41) \times 10^{-6}$	0.	0.	cm^{-1}	
δ_J	0.	0.	0.	cm^{-1}	
δ_K	$1.1(6) \times 10^{-6}$	0.	0.	cm^{-1}	
F_α	5.219 0(18)	g.s.	n.a.	cm^{-1}	b
F	7.552 4(41)	7.089 4(38)	n.a.	cm^{-1}	c
V_3	404.57(23)	592(5).	n.a.	cm^{-1}	
V_6	-9.54(20)	0.	n.a.	cm^{-1}	
η	24.96(3)	g.s.	n.a.	deg	d
ΔE_{ae}	0.069 03(35)	0.007 68(32)	-0.003 39(23)	cm^{-1}	e,f
$\Delta \nu_0^{ae}$	n.a.	-0.061 35(33)	-0.072 42(24)	cm^{-1}	g,c
ν_0^{aa}	n.a.	29 769.046(6)	29 803.420(7)	cm^{-1}	h

^a A'_a and A'_e are rigid rotor A' constants for $0a_1$ and $0e$ levels, respectively.

^b F_α is the internal rotation constant of the bare methyl group.

^c F and $\Delta \nu_0^{ae}$ are derived parameters, not used as fit variables.

^d η is the angle between the methyl top axis and the a axis.

^e ΔE_{ae} is the torsional $0a_1-0e$ splitting.

^f ΔE_{ae} is a derived parameter in the MW and 0_0^0 band fits, but a fit variable in the 14_0^1 band fit.

^g $\Delta \nu_0^{ae}$ is the distance between the origins of $0e-0e$ and $0a_1-0a_1$ subbands: $\Delta \nu_0^{ae} = \Delta E'_{ae} - \Delta E''_{ae}$.

^h ν_0^{aa} is the absolute center frequency of the $0a_1-0a_1$ subband determined by comparison with the iodine spectrum.

B. Frequency analysis: The electronic bands

The reliability of the constants determined from electronic spectra depends, apart from the number and type of lines included into the fit, on several limiting experimental factors. Most important are the experimental resolution and the linearity of the frequency scale, determined by the interferometer drift.

Since the assignments of transitions in our spectra were initially not known, the fit was performed iteratively. At first the spectrum was simulated with approximate initial constants taken from the literature.^{16,17} In each step the simulated spectrum (the composite of all the subbands) was visually compared with the observed spectrum to find new improved line assignments which were in turn used in a subsequent improved fit and simulation. The advantages of this iterative technique are outlined in our previous publications.^{19,20} Although the frequencies of $0a_1-0a_1$ and $0e-0e$ transitions are calculated separately, the χ^2 value, characterizing the quality of fit, is calculated by summing up the squared differences of observed and calculated frequencies over all the included transitions, regardless of which subband they belong to.

The correctness of the proposed assignments, given by $J', K'_a, K'_c \leftarrow J'', K''_a, K''_c$, was checked by the ground-state combination differences (GSCD). For that purpose an additional computer program was used which calculated the excited-state rotational energies from the frequencies of the assigned lines and from the known ground-state energies. For convenience we used ground-state rotational energies calculated from our microwave fit constants rather than combination differences of measured frequencies of microwave

lines. The proposed assignments are accepted only if the calculated excited-state energies for the lines, expected to share a common upper state, match within a reasonable error limit (1/3 of the observed width of electronic lines). In this way the linearity of the frequency scale is also tested.

In the frequency fits of the electronic bands, the ground-state constants (including the distortion constants) are taken from the microwave fit (Table I) and were kept fixed, while the excited-state constants were allowed to vary. Since the fixed ground-state constants define the frequency scale of the spectra more precisely than the fringes of the interferometer, a correction factor for the free spectral range of interferometer was used as a fit variable. All the calculated frequencies of electronic bands are scaled with this factor, whose deviation from unity gives a measure of the compensated systematic error of the interferometer drift. The scale correction factor was 1.000 22(5) for the origin band and 0.999 76(3) for the inversion band. The excited-state centrifugal distortion constants are all fixed to zero, since the rotationally cold electronic spectra contain only transitions with low rotational quantum numbers. Furthermore, the linewidth in the electronic spectra is about 4 orders of magnitude larger than that in the microwave spectrum.

1. The origin band

In the 0_0^0 band fit the selected variable parameters were the rotational constants A' , B' , and C' , the torsional barrier height V'_3 , the relative frequency of the band center, and the free spectral range correction factor. To achieve better con-

vergence of the fit we fixed the loosely determined fit parameters. For example, η' and F'_α were fixed to their ground-state values and V'_6 was fixed to zero.

All together 60 $0a_1-0a_1$ lines and 97 $0e-0e$ lines, characterized by the ground-state quantum numbers $J'' \leq 7$ and $K''_a \leq 2$ (except for two lines for which $K''_a = J'' = 3$), and by the transitions $\Delta K_a = 0, \pm 1$ and $\Delta J = 0, \pm 1$, were included into the final fit. The assignment of 38 $0a_1-0a_1$ lines and 89 $0e-0e$ lines were verified by GSCD.

Two moderately strong lines, assigned to c -type $0a_1-0a_1$ transitions $2,2,1 \leftarrow 2,1,1$ and $2,2,1 \leftarrow 1,1,1$, were blueshifted $\approx 0.0040 \text{ cm}^{-1}$ with respect to their frequencies predicted by the fitting program. In order to compensate this shift 0.0040 cm^{-1} was added to the calculated frequency of the $0a_1$ level with $J', K'_a, K'_c = 2,2,1$. With this correction all the line frequencies included into the fit were reproduced within 0.0031 cm^{-1} and the root-mean-square standard deviation of the fit was 0.0013 cm^{-1} .

Observed and simulated origin band spectra are presented in Fig. 3 and the molecular constants are listed in the second column of Table I. The shift of the aforementioned level has been included in the simulation. The rotational temperature and the relative subband weights used for the simulation are taken from the intensity fit described in Sec. IV C.

2. The inversion band

The fit of the 14_0^1 band with the same set of excited-state variables as for the origin band was relatively poor. The calculated $0a_1-0a_1$ lines were systematically shifted to the red and the calculated $0e-0e$ lines to the blue ($\approx 0.0034 \text{ cm}^{-1}$) in comparison to their observed positions, indicating an overestimated splitting between the predicted torsional $0a_1$ and $0e$ levels. Test fits with fixed values of the threefold barrier height V'_3 showed that the higher the barrier the better the quality of the fit. Moreover, Liu *et al.*¹⁷ found by fitting the $0a_1-0a_1$ and $0e-0e$ lines separately to a rigid asymmetric top model that the excited-state $0e$ torsional level lies below the $0a_1$ level as shown in Fig. 2. However, according to the theory of one-dimensional hindered rotation, the torsional $0e$ level must always lie higher in energy than the $0a_1$ level, i.e., $\Delta E_{ae} > 0$ for a finite threefold barrier. Since our model, which neglects the torsion-inversion coupling, cannot describe the observed ordering of torsional levels, it might be that the rigid asymmetric top model, for which the torsional $0a_1-0e$ splitting vanishes ($\Delta E'_{ae} = 0$), is a better choice for describing the rotational levels of the 14^1 state.

To mimic the rigid rotor Hamiltonian all the rotational-torsional interaction terms in the excited state Hamiltonian were disabled by fixing F'_α to zero in the fit. Since the calculated energy levels no longer depend on the barrier height V'_3 and the methyl top axis angle η' , these parameters were fixed in the fit. The variables of interest were the three rotational constants for the $0a_1$ level and another set of three rotational constants for the $0e$ level. Additionally, the torsional $0a_1-0e$ splitting $\Delta E'_{ae}$ was introduced as a fit parameter. The energies of the $0e$ level were then obtained by adding $\Delta E'_{ae}$ to the energies that resulted from the rigid rotor Hamiltonian for the $0e$ state. Indeed, the fit was improved in comparison with the fit where a finite torsional barrier was

assumed and the opposite systematic shifts of $0a_1-0a_1$ and $0e-0e$ lines were compensated by the negative value of $\Delta E'_{ae}$. Furthermore, it turned out that the B' and C' constants were nearly the same for $0a_1$ and $0e$ levels. Therefore, in order to improve the convergence of the fit, only the A' constants were assumed to be different. They are marked by A'_a and A'_e for $0a_1$ and $0e$ levels, respectively. The variables in the final fit were $A'_a, A'_e, B', C', \Delta E'_{ae}$, the relative frequency of the band center, and the correction factor of the free spectral range of the interferometer. It is important to note that the ground-state levels are still described with the nonrigid Hamiltonian (1) with the constants from the microwave fit.

All together 129 $0a_1-0a_1$ lines and 92 $0e-0e$ lines with $J'' \leq 8$, $K''_a \leq 2$, $\Delta K_a = 0, \pm 1$, and $\Delta J = 0, \pm 1$ were included into the final fit. The assignment of 125 $0a_1-0a_1$ lines and 82 $0e-0e$ lines was verified by GSCD.

Five $0a_1-0a_1$ transitions sharing a common excited state $0a_1$ level with $J', K'_a, K'_c = 1,1,1$ were found to be shifted on the average 0.0037 cm^{-1} to the red with respect to their calculated frequency. Likewise, the observed $0e$ level with $J', K'_a, K'_c = 4,0,4$ was found to be 0.0037 cm^{-1} redshifted, but the $0e$ level with $J', K'_a, K'_c = 4,1,4$ was found to be 0.0057 cm^{-1} blueshifted. Both $0e$ levels are the upper state for four identified transitions. After correcting the energies of those three levels in the fitting program all the measured line frequencies included into the fit were reproduced within 0.0031 cm^{-1} , except for the $5,3,3 \leftarrow 4,2,2$ $0e-0e$ line, whose observed position was shifted $\approx 0.0040 \text{ cm}^{-1}$ to the red. It is recognized that more excited-state levels of the inversion and the origin band are perturbed, but shifts smaller than 0.003 cm^{-1} are too small to be reliably confirmed. The root-mean-square standard deviation of the fit was 0.0012 cm^{-1} .

The observed and the simulated inversion band spectra are shown in Fig. 4. The shifts of the three aforementioned excited-state levels have been included in the simulation. The molecular constants are listed in the third column of Table I.

C. Intensity analysis

The relative intensities of the rotational transitions of the origin and inversion bands contain information which cannot be extracted from a frequency analysis only. Most important in this respect are the relative strengths of the subbands. We have performed an intensity fit of the origin and inversion band, keeping the S_0 and S_1 molecular constants obtained from the frequency fits fixed. The following parameters were allowed to vary: the rotational temperature, the vibronically induced in-plane transition dipole moment angle θ , the intensity weight factors of ab -type and c -type $0e-0e$ subbands, the background intensity, and the intensity scaling factor of the spectrum as a whole. The weight factor of the $0a_1-0a_1$ subband (c type for origin band and ab type for inversion band) was fixed to 1. The results are given in Table II.

The shape of individual lines was chosen to be Lorentzian, because this gave a better fit than a Gaussian shape. The improvement of the fits with a two-parameter Voigt shape

TABLE II. Results of the intensity fits of 0_0^0 and 14_0^1 bands: the intensities of the *ab*- and *c*-type $0e-0e$ subbands relative to the $0a_1-0a_1$ subband, the angle of the induced transition moment θ , the Lorentzian linewidth $\Delta\nu_L$, and the rotational temperature T_{rot} . The phase angle between the S_1 and S_0 threefold torsional potentials $\Delta\alpha$ is assumed to be zero in the fit; see the text.

		0_0^0 band	14_0^1 band	
$0a_1-0a_1$	<i>ab</i>	...	1	
	<i>c</i>	1	...	
$0e-0e$	<i>ab</i>	0.763(9)	0.254(4)	
	<i>c</i>	0.228(6)	0.186 6(30)	
θ		$\pm 54.61(30)$	$\pm 51.14(12)$	deg
$\Delta\nu_L$		0.011 46(8)	0.008 02(6)	cm^{-1}
T_{rot}		5.923(31)	5.979(28)	K

was too small ($\approx 1.5\%$) to justify further use of this shape. The fitted Lorentzian linewidth matches within 0.0001 cm^{-1} with the averaged width from direct measurements of fully resolved rotational lines. Narrower lines in the inversion band (measured with Ar carrier gas) in comparison with the origin band (measured with He carrier gas) are due to the lower molecular beam velocity resulting in a smaller Doppler broadening when using argon.

Apart from the Boltzmann population distribution which is characterized by a single rotational temperature, we tested two different two-temperature non-Boltzmann distributions in the intensity analysis, which are described in detail in Ref. 19. The improvement of the fit was relatively small (a few percent) for both models and was somewhat better for the inversion band. The fits resulted in nearly the same (within 1 K) rotational temperature for *J*- and *K* manifolds in contrast with earlier results of Price *et al.*,¹⁵ where the temperature for the levels with different K_a'' was found to be 10 K higher than that for levels with the same K_a'' but different *J*'. For both two-temperature distributions the weights of $0e-0e$ subband intensities as well as the induced transition dipole moment angle remained the same, differing only within their error limits.

There are still some distinct differences between the observed and simulated spectra which we note without further discussion. For example, in the region from -4.4 to -2.8 cm^{-1} of the origin band, the *b*-type $0e-0e$ lines $J-1,0, J-1 \leftarrow J,1, J$ ($J=2,3,4$) are enhanced and the *c*-type $0a_1-0a_1$ lines $J-1,0, J-1 \leftarrow J,1, J-1$ ($J=2,3,4$) are suppressed in the observed spectrum in comparison with the simulated one (see Fig. 3). In the inversion band spectrum three pairs of overlapped *b*-type $0a_1-0a_1$ lines, whose components are $J+1,3, J-1 \leftarrow J,2, J-2$ and $J+1,3, J-2 \leftarrow J,2, J-1$ ($J=2,3,4$) are clearly suppressed. The pairs corresponding to $J=2, 3$, and 4 are located at $7.1, 7.7$, and 8.3 cm^{-1} with respect to the band center, respectively (see Fig. 4).

In the intensity fits described above, the phase angle between the S_0 and S_1 torsion potentials $\Delta\alpha = \alpha' - \alpha''$ was fixed to zero. Beside this we fitted the same spectra assuming the more realistic $\Delta\alpha = 60^\circ$ phase angle by changing the sign of V_3' to negative. Unexpectedly, these fits resulted in a higher χ^2 value (37% for the origin band and 7% for the

TABLE III. Comparison of our excited-state rotational constants from the origin band fit with other author's constants who have fit the $0a_1-0a_1$ subband of the 0_0^0 band to a rigid rotor model.

	This work	Price <i>et al.</i> (Ref. 15)	Liu <i>et al.</i> (Ref. 16)	
A'	1.6019	1.596	1.6030	cm^{-1}
B'	0.3386	0.334	0.3388	cm^{-1}
C'	0.2965	0.305	0.2963	cm^{-1}

inversion band) than the fits with $\Delta\alpha = 0^\circ$, indicating poorer reproduction of the measured intensities.

V. DISCUSSION

A. Rotational constants and the rigid rotor model

Table III compares our excited-state rotational constants with those determined by Price *et al.*¹⁵ and Liu *et al.*¹⁶ from the fits of the $0a_1-0a_1$ subband of the origin band to a rigid asymmetric top model. In these fits fixed ground-state rotational constants from the microwave analysis^{1,2} were used. We note that, in spite of fact that the spectra of Price *et al.*¹⁵ were recorded with much lower resolution (≈ 0.22 vs $\approx 0.01 \text{ cm}^{-1}$ in our work), their constants still agree with our values within 0.009 cm^{-1} . The better resolution of the pulsed dye amplifier setup used by Liu *et al.*¹⁶ explains the much better agreement of their constants with ours.

The rotational energies of degenerate $0e$ species are significantly perturbed by the rotational-torsional (RT) coupling in comparison with the rigid asymmetric top energy level structure. This is governed mostly by the $-2F\rho_a p J_a$ term of the Hamiltonian (1). In the framework of perturbation theory of RT interaction²⁵⁻²⁷ this contribution can be expressed by $FW^{(1)}\rho_a K_a$, where the dimensionless first-order perturbation coefficient $W^{(1)}$ is related to the average value of the torsional angular momentum operator (the diagonal matrix element of p for a given torsional state) by $W^{(1)} = -2\langle p \rangle$.^{20,25-27} Our estimations show that for ground- and excited-state $0e$ torsional levels the factor $FW^{(1)}\rho_a$ is -0.0274 and -0.0026 cm^{-1} , respectively. Obviously, owing to the poor description of the $0e$ levels by the rigid rotor model, the analysis of $0e-0e$ lines was omitted¹⁵ or only the $0e-0e$ transitions with $K_a''=0$ and $K_a'=0,1$ were included into the fit.^{16,17} Even a model²⁰ based on fourth order perturbation theory²⁷ results in an 0.014 cm^{-1} error for the ground-state $0e$, $J'', K_a'', K_c'' = 3,3,1$ level. Therefore, we used a non-perturbative solution of the rotational-torsional problem in this study. In order to avoid problems with the ground state, Liu *et al.*^{17,18} used known ground-state energies, determined from microwave analysis, in the rigid rotor fits of the inversion band and higher electronic bands.

For nondegenerate $0a_1$ torsional levels, $W^{(1)}=0$, indicating that for these levels the first-order RT perturbation is absent.²⁵⁻²⁷ However, due to the second-order effect the constants obtained from the rigid rotor fit contain an effective contribution from the torsion. Thus, in principle, it is not thoroughly correct to compare the constants obtained from the fits to a nonrigid model with those from the fit to a rigid

rotor model. Within the second-order perturbation approach the effective and “torsion-free” A and B constants are related by

$$\begin{aligned} A_{\text{eff}} &= A + FW^{(2)}\rho_a^2, \\ B_{\text{eff}} &= B + FW^{(2)}\rho_b^2, \end{aligned} \quad (5)$$

where $W^{(2)}$ is the second-order perturbation coefficient for a given vibrational level arising from nondiagonal matrix elements of the p operator.^{20,25–27} The calculated values of $FW^{(2)}\rho_a^2$ for the $0a_1$ torsional level, being 0.0108 and 0.00087 cm⁻¹ for the ground- and excited (0^0) state of acetaldehyde, respectively, indicate a significant torsional contribution in the A''_{eff} and A'_{eff} constants. For the B''_{eff} and B'_{eff} constants this contribution is $(\rho_a''/\rho_b'')^2 = 143$ and $(\rho_a'/\rho_b')^2 = 103$ times smaller, respectively, owing to a small angle between the methyl top axis and the a axis. For the C''_{eff} and C'_{eff} constants it vanishes since $\rho_c'' = \rho_c' = 0$. These considerations explain why the value of the A' constant from the rigid rotor fit of Liu *et al.*¹⁶ is ≈ 0.001 cm⁻¹ larger than our value and why their values of the B' and C' constants are almost the same as ours (see Table III).

We also note that our absolute frequency of the $0a_1-0a_1$ subband center of the origin bands is 0.024 cm⁻¹ larger than that determined by Liu *et al.*,¹⁶ but our absolute frequency for the $0a_1-0a_1$ subband center of the inversion band matches exactly with their results.¹⁷

B. The effects of inversion

The inversion–torsion and the inversion–rotation couplings have been neglected in our model simulations. Nevertheless, the observed transitions in the origin band are well reproduced by taking into account only the rotation–torsion (RT) coupling in the excited state in the same way as in the ground state. However, this model was unsatisfactory when applied to the inversion band. Rather than using a more consistent, but very complicated, inversion–torsion–rotation model, we described the rotational levels of the 14^1 state with a simple rigid asymmetric rotor model, where different A' constants were used for the calculation of the rotational energies of the $0a_1$ and $0e$ levels, and the energies of the $0e$ level were corrected by an *ad hoc* parameter $\Delta E'_{ae}$. In this way the inversion band was also reproduced quite well. It should be noted that the formally infinite torsional barrier for the 14^1 state has nothing in common with the real potential energy surface.

Our value of the excited-state threefold barrier height for methyl torsion (592 cm⁻¹) is lower than that obtained by Liu *et al.*¹⁷ (721 cm⁻¹), Weersink *et al.*¹⁴ (680 cm⁻¹), and Baba *et al.*¹³ (691 cm⁻¹) from the torsion–inversion analysis. The difference is explainable by the fact that our V'_3 value is determined only from the rotational line frequencies of the two lowest torsional bands ($0a_1-0a_1$ and $0e-0e$ subbands of the 0_0^0 band). We did not use the available band origin data^{17,18} in our fit, because our single-large-amplitude-motion model cannot predict correctly the higher torsion–inversion levels. For example, our model cannot explain

why, for the inversion band, the $0e$ level lies beneath the $0a_1$ level. The negative $0a_1-0e$ splitting is therefore described with an extra empirical fit constant $\Delta E'_{ae}$.

The inversion motion of acetyl hydrogen in the excited state can be treated as a hindered internal rotation of the aldehyde hydrogen around the same axis (defined by the C–C bond) as the methyl group internal rotation;¹⁴ see Fig. 1. For a double-minimum inversion potential with a finite barrier all corresponding vibrational states are nondegenerate. Treating the inversion–rotation coupling within the perturbation model we can use the fact that for nondegenerate levels all the odd-order perturbation coefficients vanish to zero.^{25–27} The remaining even-order perturbation terms appear via the change of rotational constants according to Eqs. (5). Thus, within the second-order perturbation approach it is not necessary to include new terms describing inversion–rotation coupling into the rotational–torsional Hamiltonian. Since the methyl top axis makes a relatively small angle with respect to the a axis, leading to $\rho_a' \gg \rho_b'$, it is expected that the inversion–rotation coupling affects mostly the A' constant. Indeed, the rotational constants obtained from the inversion band spectrum differ from those obtained from the origin band spectrum (see Table I) and the difference is the largest (≈ -0.004 cm⁻¹) for the A' constant. A crude model calculation with a twofold sinusoidal barrier for inversion shows that the effective contribution $F'_{\text{inv}}W_{\text{inv}}^{(2)}\rho_a'^2$ [see Eqs. (5)] is positive for the 0^0 state and negative for the 14^1 state. The absolute values of $W_{\text{inv}}^{(2)}$ are nearly the same for both states. Although, this is in qualitative agreement with larger A' constant from the origin band fit, a quantitative comparison requires the use of a finer model potential.

The suppression of certain b -type $0a_1-0a_1$ lines with $K_a = 3 \leftarrow 2$ in the inversion band as noticed in Sec. IVC can be another manifestation of coupling to the inversion motion. It seems that a full understanding of the effects induced by the inversion motion can only be achieved by an analysis with a model Hamiltonian, taking the torsion–inversion as well as the rotation–inversion coupling into account.

C. Shifted energy levels

Our frequency analysis shows that some energy levels in the 0^0 as well as in the 14^1 state are shifted with respect to their expected positions. We suggest that an accidental resonance with some rovibronic level of the triplet state is responsible for these perturbations.

A possibility for such an S_1-T_1 coupling for acetaldehyde is well grounded. Gas cell fluorescence quenching experiments by collisions with oxygen³⁰ and by an external magnetic field³¹ revealed the presence of intersystem crossing to the T_1 state even for the low energy levels near the S_1 origin. Observation of the magnetic field-dependent quantum beats³² and state-selective investigations of line broadening, quantum beats, biexponential decays, and dissociation rates^{23,33,34} under free-jet conditions demonstrated an increasingly important role of intersystem crossing for the higher vibronic levels of the S_1 state.

Additional evidence of S_1-T_1 coupling for the lowest excited-state vibrational levels comes from the time-resolved

measurements.^{35,23,36} Rotationally selective lifetime measurements of Jen *et al.*³⁵ confirmed the single exponential character of decay for the lowest vibronic levels, which was observed earlier in vibrationally resolved experiments.³⁶ The lifetime of rotational levels of the 0^0 state varied in the range of 171–206 ns.³⁵ The lowest $0a_1, J', K'_a, K'_c = 0, 0, 0$ level had the shortest lifetime of 171 ns. Jen *et al.*³⁵ suggested that a perturbation by a T_1 level of the excited S_1 level can lengthen its lifetime. The rotational state-dependent variation of lifetimes can then be explained by the accidental character of perturbations. Lee and Chen²³ observed that excitation into the $0a_1, J', K'_a, K'_c = 1, 0, 1$ level of the 14^1 state resulted in an exponential decay modulated with quantum beats of 32.3 and 44.1 MHz, indicating the presence of intermediate-case S_1-T_1 coupling already at excess energy of 34 cm^{-1} .

Owing to the small (2530 cm^{-1}) S_1-T_1 separation^{37,38} the density of triplet state vibrational levels near the S_1 origin is relatively low so that S_1 levels will accidentally interact with a single T_1 level only. According to the standard nondegenerate two-level coupling scheme, the shift of perturbed level from its unperturbed position gives the estimate of the minimum possible value of the S_1-T_1 coupling matrix element. For example, for the $0e$ level of 14^1 state with rotational assignment $J', K'_a, K'_c = 4, 1, 4$ the S_1-T_1 coupling matrix element should be larger than 0.0057 cm^{-1} . We did not observe any evidence of intensity suppression for the shifted lines indicating that the S_1-T_1 mixing is not strong.

An ultimate proof for the existence of coupled S_1-T_1 pairs might be an observation of the *triplet* level rather than the singlet level of the coupled pairs. Such measurements are done for glyoxal exciting selectively into its rovibronic levels in collisionless conditions.^{39,40} The triplet-like eigenstates of the coupled S_1-T_1 pairs, called gateway states, are distinguished experimentally by their long fluorescence decay time, being an order of magnitude longer than the normal S_1 lifetime. The extreme weakness of the long-lived fluorescence from the triplet-like gateway states, which requires a special technique for its detection,^{39,40} can be a reason why the slow fluorescence is not observed yet for acetaldehyde.

D. The subband intensities

Within the Franck–Condon approximation the intensity ratio of $0e-0e$ and $0a_1-0a_1$ torsional subbands of the same type is given by

$$I_e/I_a = (g_e \cdot ns_e \cdot S_e \cdot n_e) / (g_a \cdot ns_a \cdot S_a \cdot n_a), \quad (6)$$

where g_e and g_a are the degeneracies of the $0e$ and $0a_1$ levels ($g_e = 2$ and $g_a = 1$), ns_e and ns_a are the nuclear spin statistical weights ($ns_e/ns_a = 1:2$ for molecules of G_6 symmetry), S_e and S_a are the strengths of the $0e-0e$ and $0a_1-0a_1$ torsional bands (the Franck–Condon factors), and n_e/n_a is the population ratio of the torsional levels. Under the usual assumption of the absence of collisional population redistribution between the $0a_1$ and $0e$ levels during the jet expansion, the n_e/n_a ratio is nearly 1. The intensity ratio of the Herzberg–Teller induced direct *ab*-type $0e-0e$ and $0a_1-0a_1$ subbands of the inversion band is expressed in the same way as for the direct *c*-type $0e-0e$ and $0a_1-0a_1$ sub-

bands of origin band, because in both cases the S_e/S_a ratio is determined by the torsional Franck–Condon factors.

We note that the physical meaning of the fitted subband weight factors depends on whether or not the 60° conformational change on excitation is taken into account in the intensity fit. For a given subband the intensity fit procedure matches the simulated spectrum to the observed spectrum by *scaling* it with a weight factor. If the methyl conformation is assumed to be preserved in the intensity fit, the observed subband intensities are described by the subband weight factors. In this case the ratio of the weights of the direct $0e-0e$ and $0a_1-0a_1$ subbands reflects the ratio of corresponding Franck–Condon factors S_e/S_a . On the contrary, if the methyl conformation is assumed to change in the intensity fit, the torsional Franck–Condon factors corresponding to $\Delta\alpha = 60^\circ$ are already taken into account in the simulated spectra of the subbands. Ideally, in this case the ratio of the weights of direct $0e-0e$ and $0a_1-0a_1$ subbands should be unity.

The ratio of band strength S_e/S_a can be calculated separately from known internal rotation constants (F'' and F') and barrier heights (V''_3 , V''_6 , and V'_3) with the help of pure torsional Franck–Condon overlap model. In the case that $\Delta\alpha = 0^\circ$ the calculated S_e/S_a ratio is 1.000 and in the case that $\Delta\alpha = 60^\circ$ the calculated ratio is 0.251. The observed intensity ratios for the direct subbands given in Table II (0.23 for the origin band and 0.25 for the inversion band) are close to the calculated value for $\Delta\alpha = 60^\circ$.

The intensity weights of indirect $0e-0e$ subbands given in Table II are merely empirical parameters in our model. As the indirect subbands are induced by torsion–inversion coupling, models accounting for this effect^{14,41} are required to predict their relative intensities.

Liu *et al.* concluded^{16,17,42} that the relative intensity of $0e-0e$ subbands decreases as the rotational temperature rises by comparing the excitation spectra of acetaldehyde measured at warm ($T_{\text{rot}} = 5-9 \text{ K}$) and cold ($T_{\text{rot}} \approx 0.7 \text{ K}$) jet conditions. However, a visual comparison of our simulations (with the subband weights taken from Table II and a guessed value of T_{rot}) and their published spectra^{16,17} indicates that for a given band their “cold” and “warm” spectra are reproducible (although not in details) with the *same* subband intensity weights.

The angle of the induced transition dipole moment θ is related to the strength (intensity) ratio of the *b*-type and *a*-type components of the hybrid *ab*-type $0a_1-0a_1$ and $0e-0e$ subbands by

$$\tan^2 \theta = s_b/s_a. \quad (7)$$

We note that s_a should be not confused with S_a used in Eq. (6) to mark the strength of the whole $0a_1-0a_1$ subband, which can be *ab*- as well as *c* type. As expected, the fit of the origin and the inversion bands yielded similar values for the angle of the induced transition moment. Its sign remains ambiguous, because the quantum interference effects^{43,20} are too small to distinguish opposite signs of θ compared to the experimental accuracy with which the intensities are determined. The value of this angle hopefully can help to assign the inducing higher electronic state in the near future. No evidence of axis switching (reorientation)^{44,45,19} upon elec-

tronic excitation (in the *ab* plane) was found in the *ab*-type hybrid subbands of the origin and the inversion band.

E. Methyl conformational change and relative line intensities

Under the assumption of 60° phase change between the excited- and ground-state torsional potentials the intensity fits were poorer. If the only difference between the cases with $\Delta\alpha=0^\circ$ and $\Delta\alpha=60^\circ$ were the change of torsional Franck–Condon factors, no degradation of the fit quality would be expected. The smaller predicted strength of the $0e-0e$ subbands in $\Delta\alpha=60^\circ$ case would be simply compensated by their larger weight factors. However, our simulations showed, indeed, that the relative intensities of rotational lines of a given torsional subband are different in $\Delta\alpha=0^\circ$ and in $\Delta\alpha=60^\circ$ cases. Relative intensities were changed (for some lines even by a factor of 2–5) for $0a_1-0a_1$ as well as for $0e-0e$ subbands. Usually it is assumed that the relative intensities of rotational lines are independent of the presence or absence of a conformational change. This case of acetaldehyde shows, however, that this effect should be carefully considered in analysis of electronic spectra of molecules with strong rotational–torsional coupling. More detailed investigation of this effect is in progress and the results will be published elsewhere.²⁹

It still remains unclear why the simulations, where the absence of methyl conformational change on excitation is presumed, are in better agreement with the measured spectra. Previous investigations of vibrationally resolved excitation spectra^{14,17} and also our results (Sec. VD) leave no doubt about the presence of conformational change. It could be that the optimum of the intensity fits correspond to some intermediate conformational change angle, $0^\circ < \Delta\alpha < 60^\circ$, which is not accessible in our model.

VI. SUMMARY

It is shown that all lines in the rotationally resolved spectra of the two lowest electronic bands of jet-cooled ($T_{\text{rot}} \approx 6$ K) acetaldehyde are reproduced with a model, where the interaction between the methyl torsion and the overall rotation is rigorously taken into account, but the inversion–torsion and inversion–rotation couplings are neglected. In our analysis the ground- and electronically excited states are modeled with the *same* Hamiltonian, giving the same physical meaning to corresponding excited- and ground-state constants. Moreover, this approach enabled us to predict the intensities of the lines apart from their frequencies. In the simulation of the origin band the 0^0 state was described with a finite threefold torsional barrier higher (by about 1.5 times) than the ground-state one. The inversion band could not be described with this model. Therefore, in the simulation of the inversion band, the 14^1 state was described with a rigid asymmetric top Hamiltonian and with two extra parameters (negative torsional $0a_1-0e$ splitting and a different A' constant for the $0e$ state). Shifts of some excited-state levels with respect to their predicted positions were explained by accidental couplings with nearly isoenergetic high rovibronic levels of the triplet state. The intensity fit yielded reliable

values of the relative intensities of the *ab*-type and *c*-type $0e-0e$ subbands with respect to the $0a_1-0a_1$ subband and the angle of Herzberg–Teller-induced transition dipole moment. Although the torsion–inversion analysis of the vibrationally resolved excitation spectrum firmly proves the presence of a near 60° conformational change on excitation, the observed rotational spectra are in better agreement with simulations, where the absence of conformational change is assumed.

This work is a step toward a global analysis of the excited-state data of acetaldehyde isotopomers. The ultimate goal is to fit all the frequencies and intensities of the rotational lines of different vibronic bands simultaneously to a model, which takes consistently into account the coupling between rotation, torsion, and inversion.

ACKNOWLEDGMENTS

E.J. is grateful to J. T. Hougen for valuable suggestions and to I. Kleiner for providing the microwave and far infrared data, and for testing the fitting/simulation software. A.M.W. thanks the NSF under Grant No. CHE 9726267.

- ¹R. W. Kilb, C. C. Lin, and E. B. Wilson, *J. Chem. Phys.* **26**, 1695 (1957).
- ²A. Bauder and Hs. H. Günthard, *J. Mol. Spectrosc.* **60**, 290 (1976).
- ³W. Liang, J. G. Baker, E. Herbst, R. A. Booker, and F. C. De Lucia, *J. Mol. Spectrosc.* **120**, 298 (1986).
- ⁴I. Kleiner, J. T. Hougen, R. D. Suenram, F. J. Lovas, and M. Godefroid, *J. Mol. Spectrosc.* **148**, 38 (1991).
- ⁵I. Kleiner, J. T. Hougen, R. D. Suenram, F. J. Lovas, and M. Godefroid, *J. Mol. Spectrosc.* **153**, 578 (1992).
- ⁶S. P. Belov, M. Yu. Tretyakov, I. Kleiner, and J. T. Hougen, *J. Mol. Spectrosc.* **160**, 61 (1993).
- ⁷I. Kleiner, F. J. Lovas, and M. Godefroid, *J. Phys. Chem. Ref. Data* **25**, 1113 (1996).
- ⁸I. Kleiner, J. T. Hougen, J.-U. Grabow, S. P. Belov, M. Yu. Tretyakov, and J. Cosléou, *J. Mol. Spectrosc.* **179**, 41 (1996).
- ⁹K. K. Innes and L. E. Giddings, *J. Mol. Spectrosc.* **7**, 435 (1961).
- ¹⁰L. M. Hubbard, D. F. Bocian, and R. R. Birge, *J. Am. Chem. Soc.* **103**, 3313 (1981).
- ¹¹M. Noble, E. C. Apel, and E. K. C. Lee, *J. Chem. Phys.* **78**, 2219 (1983).
- ¹²M. Noble and E. K. C. Lee, *J. Chem. Phys.* **81**, 1632 (1984).
- ¹³M. Baba, I. Hanazaki, and U. Nagashima, *J. Chem. Phys.* **82**, 3938 (1985).
- ¹⁴R. A. Weersink, D. T. Cramb, S. C. Wallace, and R. D. Gordon, *J. Chem. Phys.* **102**, 623 (1995).
- ¹⁵J. M. Price, J. A. Mack, G. v. Helden, X. Yang, and A. M. Wodtke, *J. Phys. Chem.* **98**, 1791 (1994).
- ¹⁶H. Liu, E. C. Lim, R. H. Judge, and D. C. Moule, *J. Chem. Phys.* **102**, 4315 (1995).
- ¹⁷H. Liu, E. C. Lim, C. Muñoz-Caro, A. Niño, R. H. Judge, and D. C. Moule, *J. Mol. Spectrosc.* **175**, 172 (1996).
- ¹⁸H. Liu, E. C. Lim, A. Niño, C. Muñoz-Caro, R. H. Judge, and D. C. Moule, *J. Mol. Spectrosc.* **190**, 78 (1998).
- ¹⁹G. Berden, W. L. Meerts, and E. Jalviste, *J. Chem. Phys.* **103**, 9596 (1995).
- ²⁰K. Remmers, E. Jalviste, I. Mistrik, G. Berden, and W. L. Meerts, *J. Chem. Phys.* **108**, 8436 (1998).
- ²¹S. Gerstenkorn and P. Luc, *Atlas du Spectroscopie d'absorption de la Molecule d'iode* (CNRS, Paris, 1978).
- ²²S. Gerstenkorn and P. Luc, *Rev. Phys. Appl.* **14**, 791 (1979).
- ²³S.-H. Lee and I.-C. Chen, *Chem. Phys.* **220**, 175 (1997).
- ²⁴J. T. Hougen, I. Kleiner, and M. Godefroid, *J. Mol. Spectrosc.* **163**, 559 (1994).
- ²⁵W. Gordy and R. L. Cook, *Microwave Molecular Spectra*, 3rd ed. (Wiley, New York, 1984).
- ²⁶C. C. Lin and J. D. Swalen, *Rev. Mod. Phys.* **31**, 841 (1959).
- ²⁷D. R. Herschbach, *J. Chem. Phys.* **31**, 91 (1959).
- ²⁸A. S. Huber, R. D. Gordon, S. A. Reid, and J. D. McDonald, *J. Chem. Phys.* **97**, 2338 (1992).

- ²⁹E. Jalviste, G. Berden, M. Drabbels, and A. M. Wodtke (unpublished).
- ³⁰N. Ohta and H. Baba, *J. Phys. Chem.* **90**, 2654 (1986).
- ³¹N. Ohta, T. Koguchi, T. Takemura, and I. Suzuka, *Chem. Phys. Lett.* **191**, 232 (1992).
- ³²T. Gejo, H. Bitto, and J. R. Huber, *Chem. Phys. Lett.* **261**, 443 (1996).
- ³³G.-H. Leu, C.-L. Huang, S.-H. Lee, Y.-C. Lee, and I.-C. Chen, *J. Chem. Phys.* **109**, 9340 (1998).
- ³⁴C.-L. Huang, V. Chien, I.-C. Chen, C.-K. Ni, and A.-H. Kung, *J. Chem. Phys.* **112**, 1797 (2000).
- ³⁵S.-H. Jen, T.-J. Hsu, and I.-C. Chen, *Chem. Phys.* **232**, 131 (1998).
- ³⁶M. Noble and E. K. C. Lee, *J. Chem. Phys.* **80**, 134 (1984).
- ³⁷H. Liu, E. C. Lim, C. Muñoz-Caro, A. Niño, R. H. Judge, and D. C. Moule, *J. Chem. Phys.* **105**, 2547 (1996).
- ³⁸A. Niño, C. Muñoz-Caro, and D. C. Moule, *J. Phys. Chem.* **98**, 1519 (1994).
- ³⁹Ch. Görling, E. Jalviste, N. Ohta, and Ch. Ottinger, *J. Phys. Chem. A* **102**, 10620 (1998).
- ⁴⁰J. Heldt, Ch. Ottinger, A. F. Vilesov, and T. Winkler, *J. Phys. Chem. A* **101**, 740 (1997).
- ⁴¹C. Muñoz-Caro, A. Niño, and D. C. Moule, *Chem. Phys.* **186**, 221 (1994).
- ⁴²D. C. Moule, R. H. Judge, H. Liu, and E. C. Lim, *Int. J. Quantum Chem.* **71**, 167 (1999).
- ⁴³D. F. Plusquellic and D. W. Pratt, *J. Chem. Phys.* **97**, 8970 (1992).
- ⁴⁴J. T. Hougen and J. K. G. Watson, *Can. J. Phys.* **43**, 298 (1965).
- ⁴⁵A. Held, B. B. Champagne, and D. W. Pratt, *J. Chem. Phys.* **95**, 8732 (1991).